ARTICLES

Small rings and amorphous tetrahedral carbon

Peter A. Schultz, Kevin Leung, and E. B. Stechel
Sandia National Laboratories, Albuquerque, New Mexico 87185
(Received 10 June 1998)

We apply first-principles density-functional calculations to study strain in dense amorphous tetrahedral carbon (a-tC). While the large strain present in small-ring structures, particularly three-member rings, could argue against their existence in a-tC, we demonstrate, based on energetic arguments, that strained small (three- and four-member) rings are plausible topological microstructural elements. We present two bulk carbon structures made up entirely of fourfold-coordinated atoms: the first with every atom in one three-member ring, the second with every atom in one four-member ring. Calculations show these bulk ring structures are relatively low in energy, only 0.37 and 0.23 eV/atom above diamond, respectively. This computed strain energy is much less than that present in recent models for a-tC. We examine properties of these structures with the intention to provide benchmark calculations for more approximate models, and to investigate the impact small rings might have on the properties of a-tC. We use a recently developed linear-response algorithm to compute phonon spectra for these ring structures. [S0163-1829(99)02901-X]

I. INTRODUCTION

Generating realistic, accurate model structures for amorphous tetrahedral carbon (a-tC), and understanding how that structure relates to materials properties, is an important step toward realizing the technological promise of this new material. Although much effort has been invested recently in simulations meant to generate candidate structures using semiempirical methods,[1–6] and both approximate[7] and convergent density-functional approaches,[8–10] little is definitively known about the microstructure that characterizes a-tC. For dense a-tC ($\sim$3 g/cm^3), experiments indicate a highly strained network of predominantly fourfold-coordinated (only nominally tetrahedral or sp^3), with a nonnegligible and perhaps a significant proportion of threefold coordinated (only nominally sp^2) atoms.[11–16] Simulations suggest the threefold-coordinated atoms are connected into (possibly branched) chainlike clusters of even size.[2,3,7,8] In the current work we focus on the issue of the existence of small rings in a-tC.

The bonding network in a-tC is conveniently characterized in terms of ring statistics. The topology of a-tC structures predicted from simulations is dominated by five- six- and seven-member rings,[2,3,6,8,17] near the six that characterize crystalline carbon (diamond or graphite). While some early simulations predicted no three- or four-member rings,[2,3,6] and analyses of experimentally derived radial distribution functions (RDF's) typically assume no rings smaller than five, strong evidence now supports the existence of four-member rings in a-tC. The RDF derived from the results of neutron-scattering experiments[15,16] revealed a feature near 2.1 Å, and Marks *et al.*,[8] noted this can only be explained as the distance across a diagonal in a four-member ring. Simulations by Drabold, Fedders, and Stumm[7] using a local basis density-functional[18] (LBDF) method, and Marks *et al.*,[8] have produced three-member rings. However, no experimental measurable result has yet been identified that would be specifically sensitive to three-member rings, and simulations have obtained mixed results. Hence, whether three-member rings exist in a-tC remains an unresolved question, and, furthermore, how the presence of these small rings might affect the properties of a-tC is unknown.

Determining whether these rings exist in a-tC, and how their existence affects the properties of the material is difficult. Density-functional methods can and have been used to generate structural models for a-tC (Refs. 8 and 9) and accurately reproduce experimental RDF. However, the computational requirements of a fully convergent calculation constrain the size of the amorphous unit cell as well as the length of the annealing dynamics. The number of structures that one can generate is consequently also limited. With only a small sample of small structures, one cannot ensure that predicted microstructures are not artifacts of the limited statistics or dynamics. Further advances in our understanding of a-tC will require using more approximate models, such as tight-binding molecular dynamics (TBMD), to overcome these limitations.

On one hand, recent convergent density-functional simulations using small unit cells have predicted modest numbers of three-member rings.[8,9] On the other hand, TBMD simulations, using larger unit cells and better annealing dynamics (slower cooling rates) predict far fewer three-member rings.[19] These results, coupled with the large strain embodied in such small rings, might be used to argue against the presence of three-member rings in a-tC. However, while more approximate (LBDF, TBMD, semiempirical or first-principles-based) methods can improve the quality of the annealing dynamics and allow for better statistics, they do so at the cost of reduced accuracy in structural energetics. We have previously shown that this reduced accuracy, particu-

larly in highly strained environments such as *a*-tC, can have potentially profound consequences on predicted structures.[17] For example, the proportion of threefold bonded atoms, and energetics of strain in small, particularly three-member, rings, are poorly described in methods without adequate basis set flexibility. Using first-principles local-density approximation (LDA) calculations, we showed that a minimum basis description overestimates the strain energy in cyclopropane (C_3H_6) by 0.7 eV with respect to a converged basis.[17] In calculations for a suite of hydrocarbon molecules, Porezag *et al.*,[20] found that the TBMD method, while otherwise giving excellent results, overestimates the strain energy in cyclopropane by 1.6 eV with respect to an LDA result (and experiment).

More approximate methods are required to perform adequate simulations but it is imperative that the method adopted be adequately accurate to faithfully reproduce the energetics for the full structural complexity present in *a*-tC. Rather than generating yet another limited sample of amorphous models, we adopt the approach of studying smaller crystalline systems incorporating key microstructural elements potentially present in *a*-tC. In this work we focus on small ring structures, and examine the properties of these structures in isolation. We present two crystalline carbon structures, one incorporating three-member and the other four-member rings. The strain energy in these small rings is less than might be expected, and is substantially less than the average computed strain energy in *a*-tC models generated from convergent density-functional calculations. The three-member rings are higher in energy than four-member rings, but are comparable on the scale of the background strain energy present in *a*-tC models. Thus, if four-member rings exist in *a*-tC, this suggests that three-member rings should also exist.

The bulk crystal ring structures also serve as valuable new benchmarks in testing the transferability of approximate methods, such as the tight binding method, for the generation of *a*-tC structures. Indeed, calculated properties of these structures would be a useful part of a database for refining parameters of approximate models such as the tight binding model. Here we present not only the equilibrium structures and total energies, but also the full phonon spectrum for both structures, using a recently developed linear-response algorithm.[21] The phonon spectrum provides additional benchmark data for approximate methods, describing elastic properties in these highly strained systems.

We begin in the next section with a brief account of computational details. We then discuss the energetics and bonding topology of a pair of relaxed *a*-tC models, to frame the issue of the character and magnitude of the strain energy in *a*-tC. In the following section, we present the structures and energies of the bulk ring structures, along with a sampling of other crystal structures. We examine some properties of these bulk structures, with the intent of understanding the nature of the bonding and how it relates to the bonding in *a*-tC. We close with a discussion of the importance of these models for the simulation of *a*-tC and some brief conclusions.

II. COMPUTATIONAL DETAILS

None of the structures examined in this work incorporate dangling bonds or unpaired electrons. Hence, we use the spinless local-density approximation[22] (LDA) to density-functional theory[23] in the first-principles calculations. For structural determinations and energetics we use a Gaussian-based linear combination of atomic orbitals (LCAO) method.[24] The LDA employs the Perdew/Zunger parametrization[25] of the Ceperley/Alder electron gas results,[26] and uses the generalized norm-conserving pseudopotentials (in the nonlocal form) of Hamann[27] to remove explicit treatment of the chemically inert core electrons.

TABLE I. Contracted Gaussian LCAO basis set for carbon used in this study, of the form: $\Sigma_i c_i r^l \exp(-\alpha_i r^2)$.

s function		*p* function	
α_i	c_i	α_i	c_i
5.666 238	0.436 204	4.726 973	1.695 053
2.833 119	−1.266 412	1.516 922	1.034 004
1.416 558	0.351 997	0.551 519	0.559 458
0.463 040	0.661 100	0.162 507	0.121 087
0.157 112	0.231 601		

As our study focuses on structures with fourfold-coordinated carbon atoms, the Gaussian basis sets have been optimally contracted for carbon in the diamond structure. Construction of the basis started in standard fashion with a fit to pseudoatomic orbitals, but the contraction coefficients were modified to give the best minimum basis description for diamond, i.e., best energy. This defines a reference atom. Parameters for this basis are listed in Table I. Five Gaussians are contracted to give an *s* function, four Gaussians to give a *p* function. A single *s* and *p* shell produces a minimum basis single-zeta (SZ) description of the atom: $(5s4p/1s1p)$. A double-zeta plus polarization (DZP) basis $(5s4p1d/2s2p1d)$ gives a second degree of freedom in the radial description via segmentation, by adding to the basis the longest range Gaussian of each shell, and a single Gaussian (decay constant: 0.86/bohr^2) *d* function for angular polarization. This reproduces well the detailed results of basis-converged plane-wave calculations.[28] Calculations to determine equilibrium structural parameters used a DZP basis and were converged with respect to *k*-point sampling.

For calculations of phonons in the bulk ring structures, an occupied subspace invariant linear-response algorithm is used.[21] The present implementation of this method uses a plane-wave basis.[29] These calculations employed Troullier-Martins pseudopotentials[30] and a plane-wave cutoff of 50 Ry/atom. The dynamical matrices are computed on a $4\times4\times4$ *k*-space grid, and transformed to real space to give phonon frequencies on a fine mesh. Diagonal terms are obtained variationally using a Lanczos algorithm.[21,29,31] First-order variational corrections are added to the off-diagonal terms to ensure a convergence rate similar to the diagonal terms. This algorithm gives results identical to other linear-response formulations,[32] but does not require explicit knowledge or use of stationary states in the occupied subspace. It does require having some representation of the occupied subspace.

III. AMORPHOUS TETRAHEDRAL CARBON MODELS

Large strain characterizes the bonding in *a*-tC. To establish a baseline for the energetics of strain in this study, we

start with two small (64-atom) bulk models. The first is a 2.94 g/cm^3 structure generated by Drabold, Fedders, and Stumm[7] (DFS) using a minimum basis Harris functional method,[33] and, the second, a 2.91 g/cm^3 structure from Marks *et al.*,[8] using a first-principles Car-Parrinello method.[34] Previously, we had done a full quench within our LCAO method to find (meta-)stable minimum-energy structures based on these two starting structures.[17] The two DZP-relaxed structures, besides their very different origins, had notable similarities: in the proportion of threefold atoms (near 30%), number of four-member rings, and, most strikingly, the *total* energies of the two models differed by only 0.08 eV, at 0.62 eV/atom above diamond.

The two structures, however, do differ in one important particular, the average nearest-neighbor bond length. The DFS+DZP structure has an average bond length of 1.552 Å, and the Marks+DZP structure gave 1.534 Å. Given the otherwise similar character of the structures, this difference suggests a significant difference in the average bond order of the atoms in the two lattices. We introduce a simple linear bond-length/bond-strength relation,

$$\text{bond order (atom)} = \sum_{\text{NN}} \frac{(1.74\ \text{Å} - R_{\text{NN}})}{0.20\ \text{Å}}, \qquad (1)$$

to measure the degree of bondedness about an atom. Using this formula, a nearest-neighbor distance of 1.54 Å, such as in diamond, has a bond order of exactly one, and a nearest-neighbor distance of 1.34 Å corresponds to a double bond. Any atom beyond 1.74 Å is unbonded.

The DFS+DZP structure gives an average bond order of 3.49, and 3.86 for the Marks+DZP structure. While admittedly a crude measure, this result suggests that the DFS +DZP structure is underbonded with respect to the Marks +DZP structure, and with respect to diamond (and an ideal value of 4.00). The degree to which the DFS+DZP structure is underbonded suggests that the system is under stress, and that the condition of fixed volume neglected an important degree of freedom in generating an optimal structure. Calculations varying the volume hydrostatically and relaxing the atomic coordinates upon a global scaling of the cell size confirm this hypothesis. The DFS+DZP model prefers to compress, by 1.7% in lattice parameter, to an optimal density of 3.10 g/cm^3 and an average bond order of 3.93 bonds/atom. The Marks+DZP model also compresses, by 1.0% in lattice parameter, to 3.00 g/cm^3 and 4.04 bonds/atom. Note that the average bond order relation presented in Eq. (1) functions as a rather good, if crude, figure of merit for the level of global stress in a model. The energy of both DZP-relaxed structures remained approximately 0.6 eV/atom above diamond.

The two relaxed structures have the same number of four-member rings, three, but full relaxation of the minimum-basis Harris functional DFS structure leaves only one three-member ring. The relaxed Marks structure keeps all three from the original structure. It is not necessarily true, however, that basis-converged first-principles calculations give better predictions of the real material. Because of the greater computational demands of first-principles methods, the annealing dynamics is necessarily abbreviated. The small rings might prefer to dissolve, but the length of the simulation might be inadequate to observe this event. Furthermore, supercell sizes are rather limited as well, to only 64 atoms. For this size supercell, we observe that an atom still (though weakly) interacts with its image in neighboring supercell: the LCAO basis orbitals do not have zero overlap. Certainly the strain field given by a three-member ring feels its image in the next cell, and this may cause these rings to ''crystallize,'' and make it more difficult for them to break up by trapping them in local minima. Finally, this represents a very limited sample of structures, and confident predictions are therefore not possible because of the inadequate statistics.

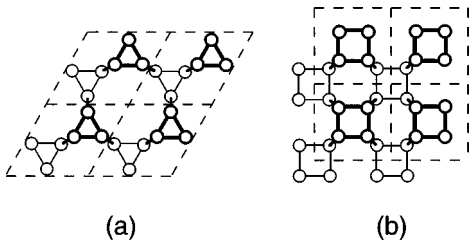

FIG. 1. Two layers of the carbon bulk ring structures, viewed from above. The dashed lines represent the unit-cell basis vectors within the plane. (a) hcp-$C3$ structure (b) bct-$C4$ structure.

Additionally, once a model is generated, it is difficult to isolate what the properties of a particular microstructural feature such as a three-member ring have *in situ*. Provided the simulation generated a model representative of *a*-tC that included three-member rings, what properties of that model are due to the ring, and what can be attributed to the local environment, different around every ring? Rather than generating yet another potentially flawed structural model, we take the approach of examining the properties of likely microstructural elements separately.

IV. BULK CRYSTAL RINGS

A. Structure

We have constructed two carbon crystal structures, designed to probe the properties of small rings in bulk carbon. In both structures, every carbon atom is fourfold coordinated. In the first structure, every atom is in exactly one three-member ring, and in the second, in one four-member ring. The first structure can be thought of as an hcp array of three-member rings, as depicted in Fig. 1(a). Hexagonal sheets of equilateral triangles are stacked vertically in an *ABAB* sequence. The triangles in the *B* sheets are rotated 60° so as to align the bonds between the sheets. We will label this structure hcp-$C3$. The second structure, labeled bct-$C4$, is also a layered structure, with planes of squares stacked to form the body-centered-tetragonal array of four-member rings shown in Fig. 1(b). The hcp-$C3$ structure belongs to space group $P6_3/mmc$ and the bct-$C4$ structure belongs to space group $I4/mmm$.

A full structural optimization within a DZP basis was performed, subject to these symmetry constraints. Three parameters define both structures. One convenient way to represent them is with the planar lattice parameter *a*, the interplanar repeat spacing *c*, and the intraring bond length. Alternatively, two bond lengths, intra- and inter-ring, and a bond angle define the structures. The optimal parameters for hcp-$C3$ and bct-$C4$ are presented in Figs. 2(a) and 2(b), in a side sche-

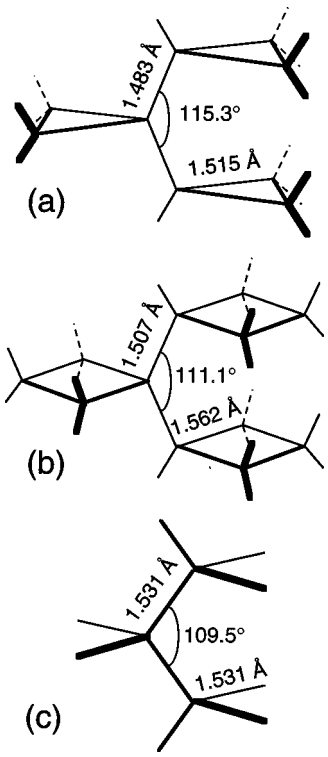

FIG. 2. Schematic side view of the local bonding in, (a) the hcp-$C3$ structure, (b) the bct-$C4$ structure, and (c) the diamond structure. The DZP optimized structural parameters are included in the figure.

matic view of the structures to emphasize the bonding topology about each atom. For comparison, the corresponding parameters for the analogous calculation for diamond are also presented, in Fig. 2(c). From this perspective, it is apparent how planes of rings, with their strained bonds, are connected by chains of relatively unstrained bonds in the z direction.

While the vertical chains are relatively unstrained, they do feel the effect of the strain within the rings in the plane. The chain bonds become progressively stronger and shorter in going from diamond to bct-$C4$ to hcp-$C3$, to make up for the loss in bond strength due to increased strain in the other intraring bonds of the atom. An examination of the charge density reveals the character of the chain bonds in these three crystals. The total charge density, however, as that for diamond presented in Fig. 3, is not very illuminating. To highlight the directional bonding character of the structures, we

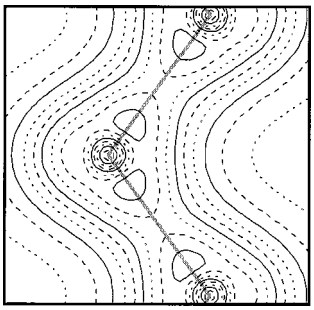

FIG. 3. Contour plot of the total charge density in diamond. The contour values increases linearly, from dot to dash to solid lines, etc. The gray lines connect the atom centers.

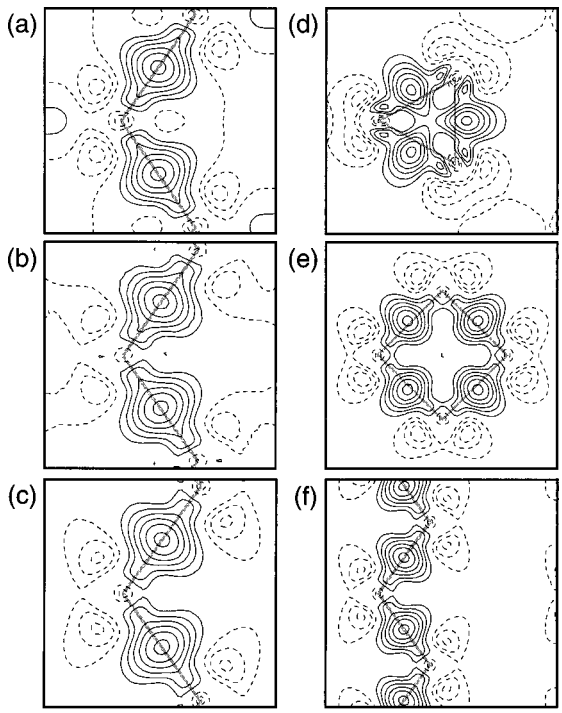

FIG. 4. Contour plots of the bond density, i.e., the total density minus the density of overlapping spherical reference atoms. Solid lines denote increased electron density, dashes the loss of electron density. (a)–(c): the bond density along the chains connecting ring planes for hcp-$C3$, bct-$C4$, and diamond, respectively. (d)–(f): the bond density in the plane of the rings for hcp-$C3$, bct-$C4$, and diamond, respectively. Again, the gray lines connect atom centers.

subtract a density given by overlapping neutral spherical reference atoms. Over the unit cell, the resulting subtracted density integrates to zero, and captures all the directional rearrangement of charge in the structure that describes the bonding.

The result along the chain bonds is presented in the contour plots of Figs. 4(a)–4(c). With a spherical background removed, the charge redistribution driven by the bonding in each of the structures reveals a buildup of density in the center of the bonds. Each mound in the bond center contains about 0.1 electrons in each of the structures. Although the chain bond lengths differ by up to 3% between these three crystals, the bond character is clearly similar.

The chain bond angles also show a systematic progression, increasing from tetrahedral in diamond to 115.3° in hcp-$C3$. The intraring bond lengths, however, do not exhibit the same trend. The intraring bond in bct-$C4$ is 2.0% longer than in diamond, while in hcp-$C3$ it is 1.0% shorter than in diamond. Bond density plots in the plane of the rings, presented in Figs. 4(d)–4(f) provide an explanation for this anomalous behavior. The bonds in four-member ring, given in Fig. 4(e), look much like the bonds in diamond, Fig. 4(f), only more tightly wound. The result for the three-member ring in Fig. 4(d), however, shows a more marked bowing of the bond outside a line connecting the atom centers, and shows a buildup of density in the middle of the ring. This stands in contrast to the (slight) loss of charge in the middle of the four-member ring in bct-$C4$ (and in diamond).

The shorter bond length in the three-member ring could, in part, be explained as a result of the bowing outwards of

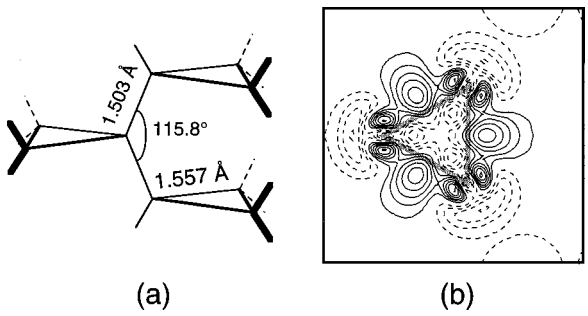

FIG. 5. The bonding in the minimum basis SZ description of the hcp-$C3$ structure. (a) The schematic representation of the local structure with structural parameters optimized using the SZ basis, cf. Fig. 2(a). (b) The bonding density in the plane of the three member ring. Note the loss of density in the center of the ring in comparison to the gain of density in the DZP description in Fig. 4(d).

the bond, and the bond length along this bowed direction being conserved. However, this implies the four-member ring should also have a shorter bond, which it does not. The buildup of charge in the middle of the three-member suggests an alternative: constructive interference of the bonds in the ring that strengthens the interaction of the bonds within the ring, thereby making shorter bonds. The six electrons of the ring bonds in hcp-$C3$ satisfy the $4n+2$ rule for a constructive interference, in much the same way that the six π electrons in benzene strengthen its bonds via resonance. The eight electrons of a four-member ring violate this rule, the interference is destructive, and the bonds are longer. Consequently, the average bond order of the bct-$C4$ structure, at 4.11 bonds/atom, is near ideal, as the shorter inter-ring bonds counterbalance the longer intraring bonds. However, with all bonds shortened, the hcp-$C3$ structure has a much larger average bond order of 4.83 bonds/atom.

This effect is made apparent when quality of basis set is considered. Our earlier work demonstrated that a minimum basis description significantly overestimates the strain energy in cyclopropane. The current work confirms that to obtain accurate results for strained microstructures requires a high-quality basis. While the diamond and bct-$C4$ equilibrium structures obtained using a SZ basis do not differ much from the converged DZP results, the hcp-$C3$ structure shows important differences, as shown in Fig. 5. The intraring bond distance in hcp-$C3$, Fig. 5(a), rather than being shorter than in diamond, is now as long as the bond in bct-$C4$. The strong bowing of the charge outside the bond line is still present. However, the bond density plot in the ring from the SZ calculation in Fig. 5(b) reveals a loss of density in the center of the ring, instead of the buildup observed for the DZP calculation, seen above in Fig. 4(d). This connects the strengthening of the ring bonds with the constructive interference. The problem in the minimum basis description is it lacks the flexibility to adequately accommodate the crowding of six electrons in such a confined area.

B. Energetics

Table II summarizes the energetics of these structures, and also lists the energies of a sampling of other carbon crystal structures, for comparison. The bulk ring structures, even with their strain, fit the pattern of lower coordination implying lower energy. Being four-coordinate structures, they are lower in energy than the six-coordinate simple cubic, the eight-coordinate bcc, and then the 12-coordinate fcc structures. The latter multicoordinate structures are several eV/atom higher than the four-coordinate structures. Interestingly, they all have zero bond order as the nearest-neighbor distances are greater than the bond cutoff (1.74 Å) given in Eq. (1).

TABLE II. Computed relative total energies of different carbon bulk crystal structures, using a high-quality DZP and SZ minimum basis. Energies are referenced to diamond, in eV/atom. The triple zeta plus polarization (TZP) calculation was performed using the DZP structure.

Structure	SZ	DZP	TZP
fcc	+5.14 eV/C	+4.64 eV/C	+4.63 eV/C
bcc	+4.98	+4.40	+4.38
sc	+2.98	+2.64	+2.63
BC8	+0.79	+0.69	+0.69
hcp-C3	+0.65	+0.38	+0.37
bct-C4	+0.28	+0.23	+0.23
Diamond	0.00	0.00	0.00

The bct-$C4$ structure is only 0.23 eV/atom higher than diamond. Despite the supposedly much larger strain, the hcp-$C3$ structure is only 0.14 eV/atom higher yet, at 0.37 eV/atom above diamond. This relatively modest increase is consistent with the analysis above concerning the stabilizing effect of the constructive interference within the three-member rings as opposed to the four-member ring.

In fact, both ring structures are much more stable than the $BC8$ structure,[35] a structure that has received attention recently in carbon as a structure to which diamond might convert under very high pressure.[36–39] The $BC8$ structure is an eight-atom bcc Bravais lattice structure, where every atom is approximately tetrahedrally coordinated. In silicon, it is a low-energy structure obtained via high-pressure cycling from the diamond structure.[35] Because of more efficient packing, the $BC8$ structure is denser than diamond. For carbon, our DZP result (defining parameters: $a_0 = 4.427$ Å, $x = 0.09428$) for the $BC8$ structure is 1.7% denser and 0.69 eV/atom higher in energy than diamond, in agreement with earlier studies.[38,39] Both the hcp-$C3$ and bct-$C4$ structures are less dense than diamond, by 21.3 and 5.3%, respectively.

Interestingly, the $BC8$ structure, with its strained packing of approximately tetrahedral atoms, is comparable in energy to the a-tC models above, with their dominantly fourfold-coordinated, approximately tetrahedral, strained bonding networks. However, both the four- *and* the three-member rings structures have much less strain energy than the bonding networks given in these a-tC models. The three-member rings have only ~60% of the average strain energy in a-tC models (0.6 eV).

This stability of three-member rings is only true with an adequately converged basis set. We optimized the same set of structures using a SZ basis set. These results are also presented in Table II. While the *relative* energies of other structures only change slightly, the SZ basis fails badly to describe the strain energy in hcp-$C3$. Now, rather than being

TABLE III. Computed electronic gap energies, in eV.

Diamond	bct-C4	hcp-C3	BC8	*a*-tC[a]	*a*-tC[b]
4.2 eV	2.3	2.3	2.4	1.3	0.5

[a]DFS+DZP relaxed structure.
[b]Marks+DZP relaxed structure.

much more stable than the average in *a*-tC, the energy of three-member rings is comparable. The minimum basis set has the same difficulty in treating the strain energy of these small rings in the bulk, as it had in molecular systems.[17] This further highlights the perils of using a minimum basis method to perform simulations of *a*-tC. The TZP results show that the DZP basis is well converged: there is negligible benefit in adding further radial flexibility to the orbitals.

C. Some properties

Given that these small rings are likely to be present in *a*-tC, we would like to know how their presence might affect the properties of the *a*-tC, and identify characteristics by which their existence could be determined. The four-member rings had a clear structural signature: the feature at 2.1 Å in RDF's between the large first and second-nearest neighbor peaks[15,16] uniquely identifies the ring.[8] The three-member rings have no such clear structural signature—its neighbor distances all lie buried under other peaks in the RDF.

Table III summarizes the computed gap energy in the four-coordinate structures. In agreement with previous work,[40] the electronic gap in diamond is computed to be 4.2 eV, and is indirect. The *BC*8 structure, though with a smaller gap of 2.4 eV, is also a good insulator, in agreement with earlier results.[38] The bulk ring structures produce similar gap energies. Both hcp-*C*3 and bct-*C*4 are good insulators (hcp-*C*3 having a direct gap at Γ), especially considering the usual LDA underestimate of gap energies. The computed gap energies in *a*-tC models are much smaller. Hence we conclude that, in the environment of *a*-tC, the presence of three- and four-member rings is unlikely to trigger defect levels in the gap, and therefore is consistent with *a*-tC. The rings are also unlikely to contribute to electron transport or conductivity. Hence, observation of small rings in *a*-tC will be difficult electronically.

Molecular analogs of the three-member rings discussed here are a common part of modern chemistry, cyclopropane (C_3H_6) being the most basic example, and [1.1.1] propellane (C_5H_6), a molecule where three three-member rings share a single edge, being a molecule that is readily synthesized.[41] Four-member rings exist in chemistry as well, but with one important distinction. The carbon ring of cyclobutane (C_4H_8) is most stable when buckled, while in bct-*C*4, the ring is constrained to be planar and square. This presents the possibility that the bct-*C*4 structure is not a stable structure, and that this array of four-member rings would prefer to distort to some lower symmetry, and lower energy, structure composed of buckled rings.

A full exploration of the possible distortions of the bct-*C*4 lattice by varying the structure directly would be a tedious proposition. We adopted a less direct but more comprehensive route made possible by recent developments in linear-response algorithms: to compute the phonon spectra, and search for the imaginary modes that indicate a structural instability. The character of such a mode, should it exist, would specify the nature of the distortion.

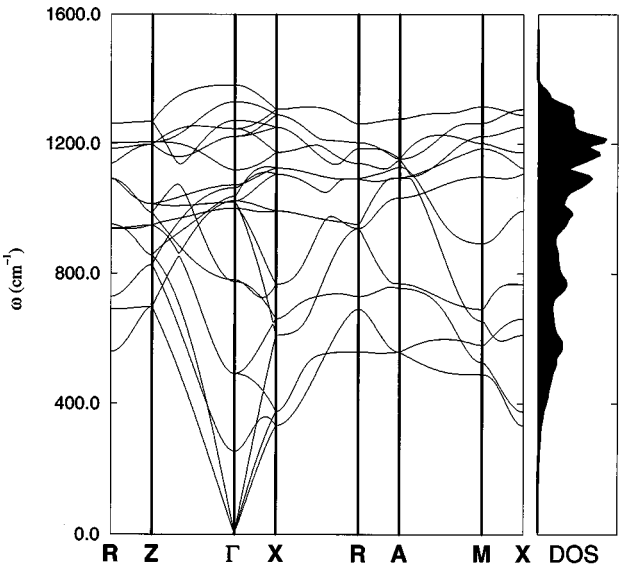

FIG. 6. Plot of the computed phonon band structure for the bct-*C*4 structure. A doubled tetragonal unit cell was used in the calculations, and thus the symmetry point symbols. The corresponding vibrational density of states is given on the right.

These calculations started with different pseudopotentials and basis than the structural determinations. As a first step, therefore, the optimal structure parameters were checked, to ensure that the atoms are at equilibrium positions. The structural differences between the LCAO results and the plane-wave results were negligible for the bulk ring structures.

The resulting phonon band structure for bct-*C*4 is depicted in Fig. 6, and that for hcp-*C*3 in Fig. 7. The bct-*C*4

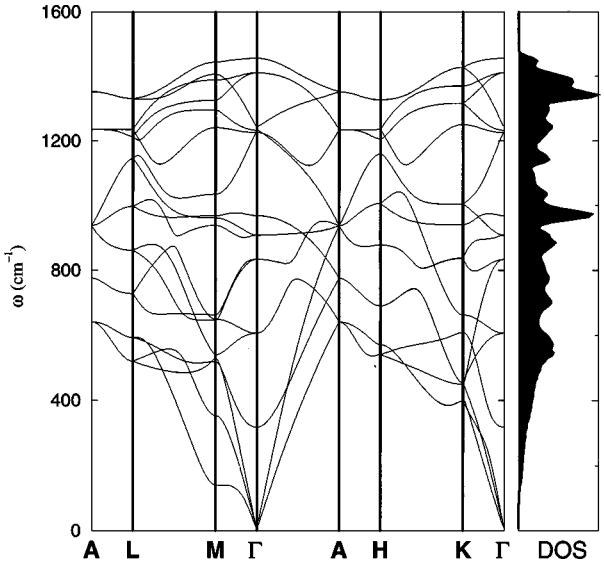

FIG. 7. Plot of the computed phonon band structure for the hcp-*C*3 structure. A hexagonal unit cell was used in the calculations, with its symmetry point symbols. The corresponding vibrational density of states is given on the right.

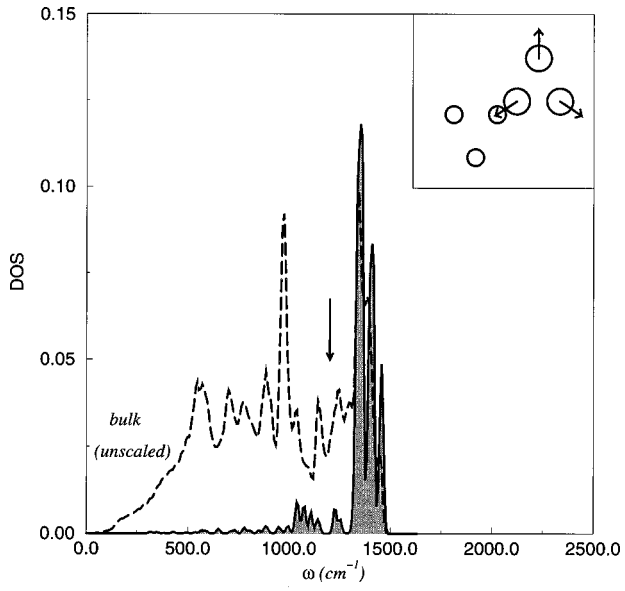

FIG. 8. Projection of one three-member ring breathing mode onto the hcp-$C3$ bulk phonon spectrum. The dashed line indicates the bulk density of states of hcp-$C3$; the shaded spectrum indicates single ring breathing mode density of states (illustrated in inset). The y axis has been rescaled. The arrow indicates breathing mode frequency of cyclopropane.

spectrum was computed in the eight-atom tetragonal unit cell (rather than the four-atom body-centered-tetragonal cell). The calculation yields no imaginary modes for bct-$C4$. Therefore, bct-$C4$ is stable against structural distortions, and the rings, unlike in the molecule, do not buckle. Unsurprisingly, hcp-$C3$ is also stable, exhibiting no imaginary modes.

The spectra are otherwise unremarkable, except in one respect. The strain in the rings should, in principle, correspond to larger effective force constants, and hence, increased vibrational frequencies, particularly for the three-member rings. In Fig. 8, the ring-stretch breathing-mode vibration of a single three-carbon ring is projected onto the bulk phonon density of states, holding all other atoms fixed. As expected, the intraring density of states dominates the high-energy portion of the spectrum. The weight of the projected spectrum is concentrated in three peaks centered at 1350, 1410, and 1450 cm^{-1}. Thus, a major portion of the ring-stretch vibrational density of states lies above the top of the entire bct-$C4$ phonon spectrum, as well as that of diamond.[42] For comparison, LDA predicts the ring-stretch frequency of cyclopropane to be $\sim$1200 cm^{-1}, in good agreement with experiments.[43] Therefore, embedding the three-member carbon ring in a carbon host increases its ring-stretch frequency significantly.

This feature holds out a (perhaps weak) possibility of finding a vibrational signature of three-member rings in a-tC through infrared or ultraviolet Raman measurements. The other less strained parts of the dominantly fourfold lattice will contribute to vibrational frequencies lower than the characteristic frequency of three-member rings, while the modes deriving from the double bonded threefold atoms, with their strong cross sections, scatter with higher frequencies.

V. DISCUSSION

Approximate methods, such as LBDF (Ref. 18) or the tight-binding method,[2,3] are typically tested and refined against a suite of molecules or clusters,[20] or a small sampling of high-symmetry bulk carbon crystal structures,[7] diamond, graphite, simple cubic, fcc, bcc, etc., and compared to accurate first-principles benchmarks. It is unclear how well the results for small hydrocarbons or carbon clusters carry over to bulk systems. It is very clear, however, that the high-symmetry structures typically used to validate methods do not probe well the transferability of a method to the highly strained, anisotropic local environments present in a-tC. The six-, eight-, and 12-coordinated atoms of the sc, bcc, and fcc/hcp structures are, at best, rarities in a-tC, and furthermore, the atoms in these crystals are located in highly isotropic sites. The various high-coordinated metallic crystal structures are all much higher in energy than the average in a-tC. In fact, we find the simple cubic structure is not even a metastable structure for carbon. It is unstable to a tetragonal distortion forming four-member rings, the bonding topology of the bct-$C4$ structure. Fixing the unit-cell dimensions at the simple cubic optimum, our calculations demonstrate that this transformation occurs with no energy barrier.

Arguably, even reproducing correctly a graphite reference has little value in demonstrating the reliability of a method for generating a-tC models. No simulations have produced aromatic microstructures in published models,[5] and are unlikely to given the high atom density of a-tC. Fourfold-coordinated structures such as $BC8$, and structures with threefold atoms and double bonds serve as better tests of transferability. The bct-$C4$ and hcp-$C3$ structures presented here, with their local anisotropy, should be particularly good systems to test and validate the ability of a method to treat highly strained environments, and a method intended to predict the populations of small rings should be able to reproduce the energetics of these reference structures accurately. An important figure of merit for approximate methods should be how well they can reproduce the detailed results—structure, energies, and phonons—provided in this paper as benchmarks.

Our calculations above show that a minimum basis method will fail this test for hcp-$C3$. Indeed, semiempirical methods such as the tight binding method may do better for these strained systems than ostensibly better first-principles based methods constrained to a minimum basis. Despite being effectively minimum-basis methods, tight-binding schemes have more adjustable degrees of freedom, due to the ability to fit matrix elements to obtain the desired results. Good results for these reference structures has been demonstrated[44] using a tight-binding method.[45]

The population of small rings in a-tC and particularly of three-member rings, will be sensitive to the energetics of the atoms in those rings, which in turn will be sensitive to the quality of the calculation. This work has shown that the strain energy in three-member rings is modest in comparison to the average strain energy present in a-tC models. Four-member rings are only slightly lower energy, and experimental evidence supports their existence. Therefore, three-member rings are also likely to be relatively common. However, if the strain energy is significantly overestimated,

as in a minimum basis calculation or inadequately transferable tight-binding method, the predicted population of these rings will be significantly reduced, perhaps even eliminated. To make reliable predictions of ring populations requires being able to compute accurately the relative energetics of various microstructural elements that compose a-tC. Other structural elements, without similar artificial energetic handicap, will gain a greater proportion of atoms in a simulation at the expense of three-member rings. While energetics are clearly not the sole consideration determining the composition of a-tC (kinetic effects play a large role), they are an important factor.

The structural properties of the ring structures reveal no new feature that could be used to identify the three-member rings in a-tC in the same way that four-member rings have been identified. Nor is there an obvious electronic signature. However, the strain in the rings leads to high-frequency features in the phonon spectrum that can be associated with these rings, and the three-member rings vibrations are located in a frequency range where it might be possible to identify them in a-tC.

Treating large strain and small rings accurately may be difficult in approximate methods. However, for the purposes of probing many properties of the material, the presence and number of three-member rings may not be important. For example, the rings are predicted to be electronically inert, as the crystals all have large energy gaps. The conductivity, electron transport, emission, and other electronic properties are likely to be dominated by the proportion and connectivity of threefold-coordinated carbon atoms. One model based on conjugated π-bonded chains of threefold bonded atoms has been shown to be consistent with the change in resistivity as a function of annealing.[46] The small rings likely serve merely as part of a general dielectric background (with relatively large gap) of four-coordinated carbon atoms, from which it will be difficult to electronically distinguish atoms in the strained rings. It still remains to be proven, however, that they are not critical for determining important structural characteristics such as the density, or compressibility.

VI. CONCLUSIONS

We have presented two carbon crystal structures composed of small rings. The atoms in three-member rings, as strained as they are, have lower energies than the average atom in current predicted a-tC structures. These results demonstrate that both four- and three-member rings are likely to be common microstructural elements in a-tC based on energetic arguments. While high-quality calculations show the three-member rings to be quite plausible energetically in a-tC, we have shown that a calculation using inadequately justified approximations, such as a minimum basis treatment, can cause errors large enough in the strain energy so as to render the three-member rings unfavorable in a-tC. Semiempirical methods should be able to demonstrate they can handle highly strained structures such as three-member rings in a-tC in order to make reliable predictions of relative populations of these rings in simulations. The two small-ring bulk structures presented here offer useful benchmarks to test and refine more approximate methods such as the tight-binding method. The greater flexibility in modifying matrix elements in TBMD offers the possibility that these semiempirical methods can be superior to minimum basis first-principles methods in treating these small rings. The computed phonon spectra offer more benchmark data for validating methods, and reveal a feature that can be used to potentially identify experimentally three-member rings in a-tC.

ACKNOWLEDGMENTS

Sandia is a multiprogram laboratory operated by the Sandia Corporation, a Lockheed Martin Company, for the United States Department of Energy, under Contract No. DEAC0494AL85000. We thank Dr. D. B. Drabold for providing the coordinates of their LBDF a-tC structure and Dr. N. A. Marks for providing the coordinates of their structure. We also thank Dr. J. P. Sullivan, Dr. M. P. Siegal, and Dr. D. R. Tallant for helpful discussions.

[1] P. C. Kelires, Phys. Rev. Lett. **68**, 1854 (1992); Phys. Rev. B **47**, 1829 (1993); Phys. Rev. Lett. **73**, 2460 (1994).

[2] C. Z. Wang and K. M. Ho, Phys. Rev. Lett. **71**, 1184 (1993); J. Phys.: Condens. Matter **6**, L239 (1994); Phys. Rev. B **50**, 12 429 (1994).

[3] Th. Frauenheim, P. Blaudeck, U. Stephan, and G. Jungnickel, Phys. Rev. B **48**, 4823 (1993).

[4] U. Stephan, Th. Frauenheim, P. Blaudeck, and G. Jungnickel, Phys. Rev. B **50**, 1489 (1994).

[5] C. H. Lee, W. R. L. Lambrecht, B. Segall, P. C. Kelires, Th. Frauenheim, and U. Stephan, Phys. Rev. B **49**, 11 448 (1994).

[6] B. R. Djordjevic, M. F. Thorpe, and F. Wooten, Phys. Rev. B **52**, 5685 (1995).

[7] D. A. Drabold, P. A. Fedders, and P. Stumm, Phys. Rev. B **49**, 16 415 (1994).

[8] N. A. Marks, D. R. McKenzie, B. A. Pailthorpe, M. Bernasconi, and M. Parrinello, Phys. Rev. Lett. **76**, 768 (1996); Phys. Rev. B **54**, 9703 (1996).

[9] D. A. Drabold, P. A. Fedders, and M. P. Grumbach, Phys. Rev. B **54**, 5480 (1996).

[10] S. J. Clark, J. Crain, and G. J. Auckland, Phys. Rev. B **55**, 14 059 (1997).

[11] J. J. Cuomo, J. P. Doyle, J. Bruley, and J. C. Liu, J. Vac. Sci. Technol. A **9**, 2210 (1991).

[12] D. J. H. Cockayne and D. R. McKenzie, Acta Crystallogr., Sect. A: Found. Crystallogr. **A44**, 870 (1988).

[13] S. D. Berger, D. R. McKenzie, and P. J. Martin, Philos. Mag. Lett. **57**, 285 (1988).

[14] D. R. McKenzie, D. Muller, and B. A. Pailthorpe, Phys. Rev. Lett. **67**, 773 (1991).

[15] P. H. Gaskell, A. Saeed, P. Chieux, and D. R. McKenzie, Phys. Rev. Lett. **67**, 1286 (1991); Philos. Mag. B **66**, 155 (1992).

[16] K. W. R. Gilkes, P. H. Gaskell, and J. Robertson, Phys. Rev. B **51**, 12 303 (1995).

[17] P. A. Schultz and E. B. Stechel, Phys. Rev. B **57**, 3295 (1998).

[18] O. F. Sankey and D. J. Niklewski, Phys. Rev. B **40**, 3979 (1989).

[19] Th. Frauenheim, G. Jungnickel, Th. Köhler, P. Sitch, and P. Blaudeck, *Proceedings of the 1st International Conference on Amorphous Carbon* (World Scientific, Singapore, 1998).
[20] D. Porezag, Th. Frauenheim, Th. Köhler, G. Seifert, and R. Kascher, Phys. Rev. B **51**, 12 947 (1995).
[21] E. B. Stechel (unpublished).
[22] W. Kohn and L. J. Sham, Phys. Rev. **140**, A1133 (1965); see, also, *Theory of the Inhomogeneous Electron Gas*, edited by S. Lundqvist and N. M. March (Plenum, New York, 1983).
[23] P. Hohenberg and W. Kohn, Phys. Rev. **136**, B864 (1964).
[24] P. A. Schultz and P. J. Feibelman, SeqQuest Program (unpublished); for a description of the method, see, P. J. Feibelman, Phys. Rev. B **35**, 2626 (1987).
[25] J. Perdew and A. Zunger, Phys. Rev. B **23**, 5048 (1981).
[26] D. M. Ceperley and B. J. Alder, Phys. Rev. Lett. **45**, 566 (1980).
[27] D. R. Hamann, Phys. Rev. B **40**, 2980 (1989).
[28] J. S. Nelson, E. B. Stechel, A. F. Wright, S. J. Plimpton, P. A. Schultz, and M. P. Sears, Phys. Rev. B **52**, 9354 (1995).
[29] K. Leung and E. B. Stechel (unpublished).
[30] N. Troullier and J. L. Martins, Phys. Rev. B **43**, 1993 (1991).
[31] J. K. Cullum and R. A. Willoughby, *Lanczos Algorithms for Large Symmetric Eigenvalue Computations* (Birkhäuser, Boston, 1985), Vols. 1 and 2.
[32] P. Giannozzi, S. de Gironcoli, P. Pavone, and S. Baroni, Phys. Rev. B **43**, 7231 (1991); X. Gonze, D. C. Allan, and M. P. Teter, Phys. Rev. Lett. **68**, 3603 (1992); X. Gonze, Phys. Rev. B **55**, 10 337 (1997); X. Gonze and C.-Y. Lee, *ibid.* **55**, 10 355 (1997).
[33] J. Harris, Phys. Rev. B **31**, 1770 (1985).
[34] R. Car and M. Parrinello, Phys. Rev. Lett. **55**, 2471 (1985).
[35] R. H. Wentorf, Jr. and J. S. Kaspar, Science **139**, 338 (1963); J. S. Kaspar and S. M. Richards, Acta Crystallogr. **17**, 752 (1964).
[36] M. T. Yin, Phys. Rev. B **30**, 1773 (1984).
[37] R. Biswas, R. M. Martin, R. J. Needs, and O. H. Nielsen, Phys. Rev. B **30**, 3210 (1984).
[38] S. Fahy and S. G. Louie, Phys. Rev. B **36**, 3373 (1987).
[39] J. Crain, S. J. Clark, G. J. Ackland, M. C. Payne, V. Milman, P. D. Hatton, and B. J. Reid, Phys. Rev. B **49**, 5329 (1994).
[40] M. T. Yin and M. L. Cohen, Phys. Rev. B **24**, 6121 (1981).
[41] K. B. Wiberg and F. H. Weller, J. Am. Chem. Soc. **104**, 15 239 (1982).
[42] P. Pavone, K. Karch, O. Schütt, W. Windl, D. Strauch, P. Giannozzi, and S. Baroni, Phys. Rev. B **48**, 3156 (1993).
[43] M. Boero and W. Andreoni, Chem. Phys. Lett. **265**, 24 (1997).
[44] M. J. Mehl (private communication).
[45] D. A. Papaconstantopoulos, M. J. Mehl, S. C. Erwin, and M. R. Pederson, in *Tight-Binding Approach to Computational Materials Science*, edited by P. E. A. Turchi, A. Gonis, and L. Columbo, MRS Proceedings No. 491 (Material Research Society, Warrendale, PA, 1998).
[46] J. P. Sullivan, T. A. Friedman, R. G. Dunn, E. B. Stechel, P. A. Schultz, M. P. Siegal, and N. Missert, in *Covalently Bonded Disordered Thin Film Materials*, edited by M. P. Siegal, W. I. Milne, and J. E. Jaske, MRS Symposia Proceedings No. 498 (Materials Research Society, Warrendale, PA, 1998), p. 97.